Islamic Azad University

Journal of

Optoelectronical Nanostructures

Winter 2024 / Vol. 9, No. 4

Research Paper

Effect of dielectric constant on the plasma characteristics of a dielectric barrier discharge reactor

Noushin Dadashzadeh*

Assistant Professor, Department of Electrical Engineering Aras Branch, Islamic Azad University, Jolfa, Iran

Received: **20 Aug. 2024**
Revised: **11 Oct. 2024**
Accepted: **30 Oct. 2024**
Published: **15 Nov. 2024**

Keywords:
Dielectric barrier Discharge (DBD), Dielectric constant , Plasma characteristics, Numerical simulation, Electron density

Abstract:

This research investigates the effect of dielectric constant variations of insulating materials on the plasma characteristics of a dielectric barrier discharge reactor at atmospheric pressure. Numerical simulations demonstrate that changes in the dielectric constant can significantly influence the spatial distribution of the plasma, electric field strength, and other key discharge parameters. The results of this study are crucial for the optimal design of DBD reactors in a wide range of applications, including plasma processing, ozone generation, and water treatment.

Citation: Noushin Dadashzadeh, Effect of dielectric constant on the plasma characteristics of a dielectric barrier discharge reactor. **Journal of Optoelectronical Nanostructures. 2024; 9 (4): 55- 68. DOI: 10.30495/JOPN.2024.33727.1329**

***Corresponding author:** Noushin Dadashzadeh
Address:
.**Tell:**09144925392 **Email:** noushin.dadashzadeh@iau.ac.ir

INTRODUCTION

Cold plasma is a state of matter generated by applying an electrical source to a gas. In this state, the gas becomes partially or fully ionized, containing particles such as free electrons, free radicals, ions, and excited atoms [1]. In cold plasma, electrons accelerated by the applied electric field collide with gas molecules, leading to ionization, excitation, or dissociation. These collisions result in the release of secondary electrons from the electrode surfaces, which are accelerated towards the cathode and reinforce the ionization process. This self-sustaining mechanism gives rise to a stable plasma [2]. One of the defining characteristics of plasma is the exceptionally high temperature of its electrons, which can reach temperatures as high as 10^5 degrees Celsius. This temperature imbalance is the defining characteristic of cold plasma and the reason for its name [3].

(DBD)[1] reactors have emerged as powerful tools for generating cold plasmas and find diverse applications including air purification, surface coating, and plasma medicine [4-9]. In these reactors, an alternating electric field is applied between two electrodes separated by one or more dielectric layers. This electric field induces localized plasma discharges where various chemical reactions occur. One of the key parameters that directly influences the performance and characteristics of these reactors is the dielectric constant of the insulating materials placed between the electrodes. The dielectric constant, defined as a measure of a material's ability to store electrical energy, directly affects the electric field distribution, plasma formation, and other physical phenomena within the DBD reactor [10].

In this research, the impact of variations in the dielectric constant of insulating materials on the plasma characteristics generated in a DBD reactor has been investigated using a detailed numerical simulation model. By altering the dielectric constant value in the simulation model, the induced changes in the spatial distribution of plasma, electric field intensity, electron density, electron temperature, and other key discharge parameters have been analyzed. To achieve the research objective, the dielectric permittivity was varied within a range of 8 to 12.

[1] Dielectric barrier discharge

1. MATH

To accurately estimate the equivalent capacitances in a parallel-plate (DBD) reactor, two equations are used to calculate the capacitance of the dielectric barrier, C_d, and the capacitance of the discharge gap, C_g. These equations are respectively as follows [11]:

$$C_g = \frac{\varepsilon_0 k_1 A}{d_g} \quad (1)$$

$$C_d = \frac{\varepsilon_0 k_2 A}{d_b} \quad (2)$$

Equation (3) calculates the gas voltage $V_g(t)$ based on the dielectric constants, the plasma area A, the dielectric thickness d, and the permittivity of free space (ε_0).

$$V_g(t) = V_e(t)\frac{C_d}{C_d + C_g} \quad (3)$$

Where $V_e(t)$ represents the external excitation voltage.

Electron density and average energy in the plasma can be calculated using an equivalent electrical network model and solving diffusion-drift equations.

$$\frac{\partial}{\partial t}(n_e) + \boldsymbol{\nabla} \cdot n_e[-(\mu_e \cdot \boldsymbol{E}) - D_e \cdot \boldsymbol{\nabla} n_e] = R_e \quad (4)$$

$$\frac{\partial}{\partial t}(n_\varepsilon) + \boldsymbol{\nabla} \cdot [-(n_\varepsilon(\mu_\varepsilon \cdot \boldsymbol{E}) - D_\varepsilon \boldsymbol{\nabla} n_\varepsilon] + \boldsymbol{E} \cdot \Gamma_e = R_\varepsilon \quad (5)$$

Equations 4 and 5 introduce the electron density n_e, diffusion coefficient D_e, source term R_e, flux Γ_e, and energy terms ($\boldsymbol{E} \cdot \Gamma_e$ and R_ε). The electron flux is driven by both the applied electric field and density gradients. The term $\boldsymbol{E} \cdot \Gamma_e$ quantifies the energy transferred to electrons from the electric field, while $R_\varepsilon$represents energy losses due to inelastic collisions as calculated in equation 6 [12].

$$R_\varepsilon = S_{en} + \frac{Q + Q_{gen}}{q} \quad (6)$$

In which S_{en} is the power loss, Q_{gen} is the total heat generation rate per unit volume, and q is the electron charge [12]. Convective effects of electrons are neglected.

Electron diffusion, energy dynamics, and energy diffusion are calculated from the following relations:

$$D_e = \mu_e T_e \quad (7)$$

$$\mu_\varepsilon = 5/3\mu_e \quad (8)$$

$$D_\varepsilon = \mu_\varepsilon T_e \quad (9)$$

In a system characterized by M reactions governing electron population dynamics and a considerably larger number of inelastic electron collisions P, the electron source term can be generally defined as [13]:

$$R_e = \sum_{j=1}^{M} x_j\, k_j N_n \quad (10)$$

The symbols x_j, k_j, and N_n respectively denote the mole fraction of the target species in the jth reaction, the corresponding rate coefficient (in units of m^3/s), and the total neutral number density (in units of m^{-3})

$$R_\varepsilon = \sum_{j=1}^{P} x_j\, k_j N_n n_e \Delta\varepsilon_j \quad (11)$$

where $\Delta\varepsilon_j$ represents the energy loss of reaction j. By integrating the expression derived from Equation (12) over the cross-section data, we can determine the rate coefficients:

$$k_k = \gamma \int_0^\infty \varepsilon\, \sigma_k(\varepsilon) f(\varepsilon) d\varepsilon \quad (12)$$

where $\gamma = \sqrt{2q/m_e}$ The equation includes the electron mass m_e, energy ε, collision cross section σ_k, and electron energy distribution function f.

The equation below allows us to determine the electrostatic field:

$$-\nabla \cdot \varepsilon_0 \varepsilon_r \nabla V = \rho \quad (13)$$

ε_0 the permittivity of vacuum, and ε_r the relative permittivity, are used in this equation.

Equation (14) calculates charge density ρ, taking into account the specific plasma chemistry outlined in the model.

$$\sum_s q_s n_s = e(Z n_i - n_e) \quad (14)$$

where q_s indicates the ionization state of particle s, Z is the atomic number, and n_i refers to the concentration of ions.

2. Boundary Conditions

When an electron collides with a wall, it can lose energy and become absorbed by the wall surface. This phenomenon is known as electron absorption. Additionally, the electron can interact with the atoms of the wall, causing changes in their atomic structure and resulting in the loss of the primary electron. In some cases, an electron collision with the wall can cause other electrons to be ejected from the wall surface and launched into the chamber. This phenomenon is called secondary emission. The kinetic energy of the primary electron must be sufficient to detach other electrons from the wall surface. Equations 15 and 16 precisely describe how the electron flux changes as a result of these physical phenomena. These equations typically include terms that describe the rate of electron absorption, the rate of production of new electrons, and also the flux of electrons moving towards the wall [12]:

$$\mathrm{n} \cdot \Gamma_e = (1/2) V_{e.th} n_e - \sum_P \gamma_P (\Gamma_P . \mathrm{n}) \quad (15)$$

By solving equation 16,

$$\mathrm{n} \cdot \Gamma_\varepsilon = (5/6) V_{e.th} n_\varepsilon - \sum_P \varepsilon_P \gamma_P (\Gamma_P . \mathrm{n}) \quad (16)$$

The additional electrons produced via secondary emission are quantified by the second term on the right-hand side of equation (15). The symbol γ_P and $V_{e.th}$ represents the secondary emission coefficient, and denotes the thermal velocity of electrons. The energy flux associated with secondary emission is represented by the second term in equation (16), where ε_P is the average energy of the secondary electrons.Regarding heavy particles, ions, due to their larger mass compared to electrons, are less influenced by electric fields. Surface charge accumulation can also affect the potential distribution near the surfaces and consequently influence the motion of both electrons and ions.

$$n \cdot (D_1 - D_2) = \rho_s \tag{17}$$

Equation (17) provides the differential equation that we solve to find the surface charge density ρ_s distributed across the surfaces.

$$\frac{d\rho_s}{dt} = n \cdot J_i + n \cdot J_e \tag{18}$$

Equation (18) defines the normal components of the total ion and electron current densities at the boundary, denoted by $n \cdot J_i$ and $n \cdot J_e$.

3. Simulation Results

Given that the discharge gap in the studied DBD reactor is significantly smaller than the dimensions of the electrode plates, a one-dimensional modeling approach is adopted for simplicity in analysis. By extending the one-dimensional solution to two dimensions (adding the time dimension) and employing the finite element method and the one-dimensional parametric extraction technique (3D visualization of one-dimensional results), the ability to examine changes in various parameters over time is enabled.

This research examined the effects of varying dielectric barrier constants from 8 to 12 on the physical profiles of a DBD reactor operating at a 740-volt, 51Hz

sinusoidal voltage.

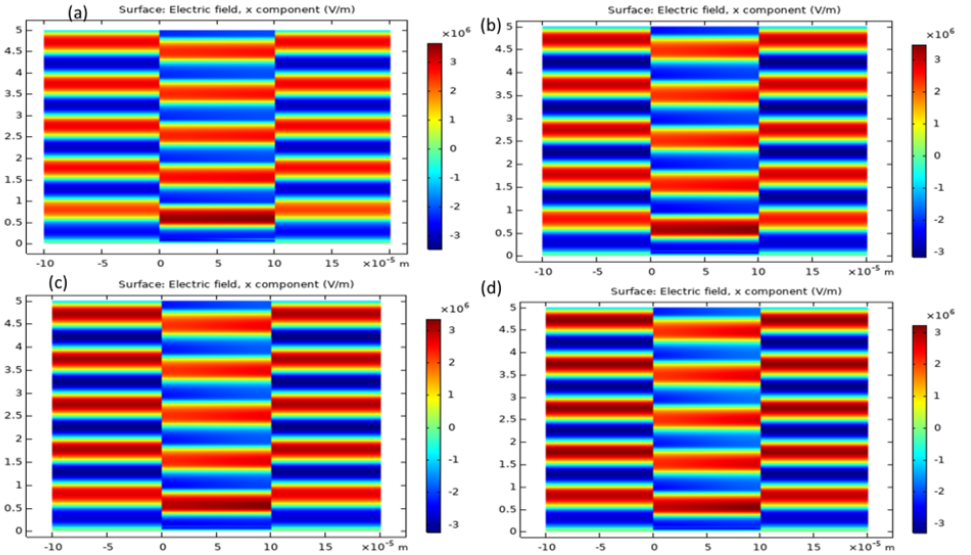

Figure 1. Electric field strength as a function of distance (x-axis) versus time (y-axis) for various dielectric constants: (a) dielectric constant of 6, (b) dielectric constant of 8, (c) dielectric constant of 10, and (d) dielectric constant of 12.

As observed in Figure 1, the electric field within the dielectric material is considerably stronger than in the discharge region. The reason for this is that the surface charges on the dielectric plates hinder the complete penetration of the electric field into the dielectric material, causing the electric field intensity within the dielectric to be lower than in the discharge region. In essence, the surface charges act as a shield, preventing the electric field from fully entering the dielectric material.

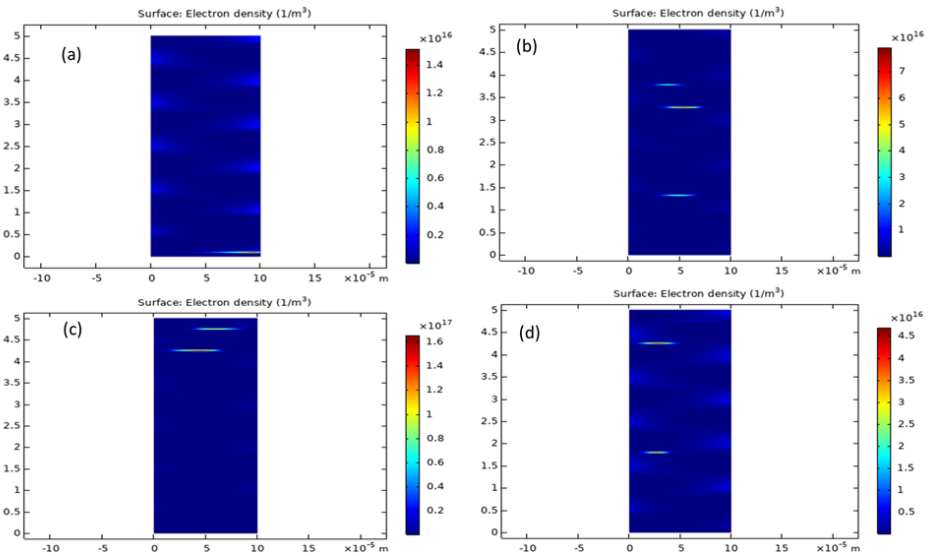

Figure 2: shows electron density profiles in the discharge area for different dielectric constants from 6 to 12.

Figure 2 shows two electrical discharges per voltage cycle, one in each half-cycle. Increasing the dielectric constant from 6 to 12 significantly increases the maximum electron density within the discharge region to approximately$16^{10}$to 17^{10} electrons per cubic meter.

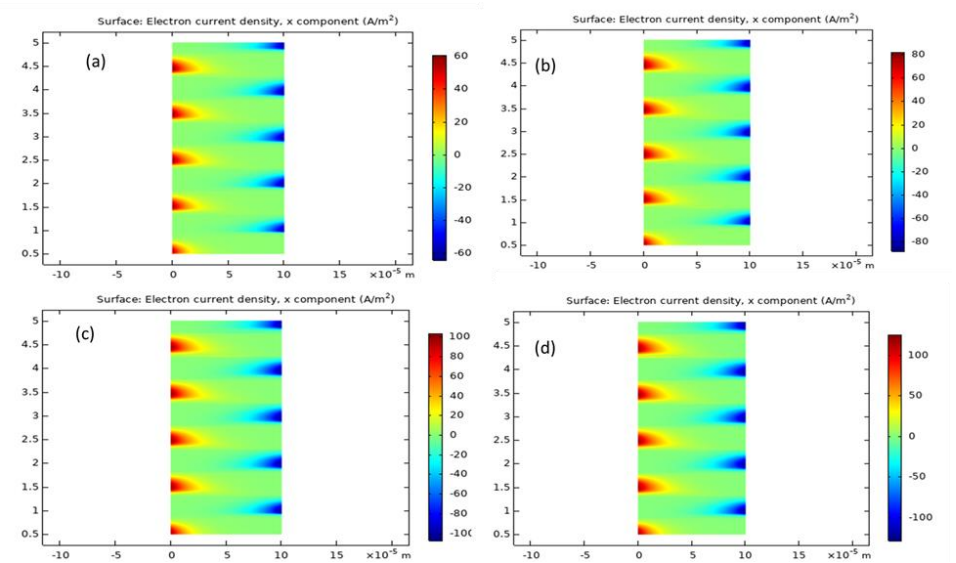

Figure 3 plots the correlation between the electron current density profiles and the dielectric constant, showcasing data for values of 6, 8, 10, and 12.

The dielectric constant directly influences electron current density, as demonstrated in Figure 3. A higher dielectric constant results in increased electron current density, thereby improving plasma conductivity.

A higher dielectric constant signifies increased material polarization. This polarization induces an electric field that opposes the external field The decrease in the effective electric field results in increased electron mobility. Electrons can move more freely within the material. Enhanced electron mobility corresponds to a higher electrical current density.

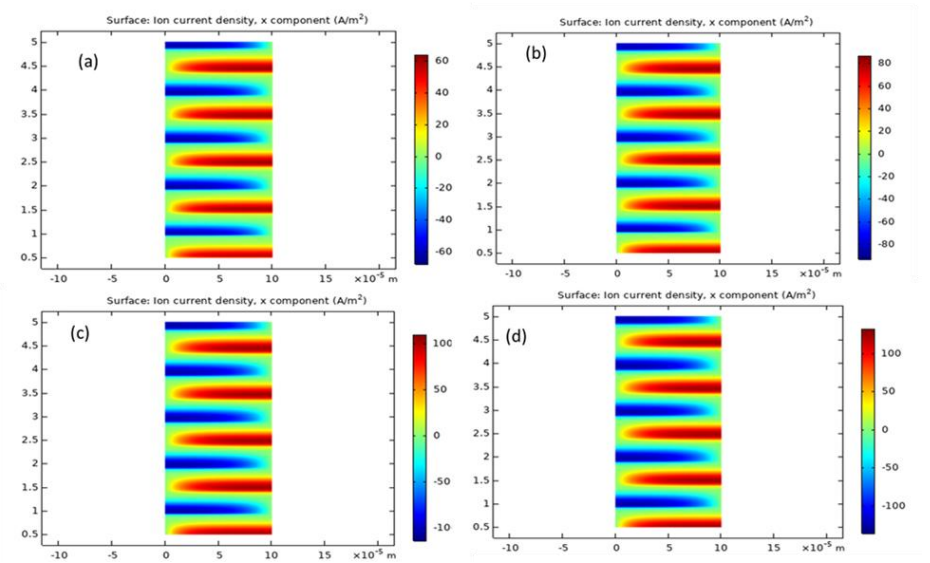

Figure 4: A comparison of ion current density profiles across the discharge gap for various dielectric constants from 6 to 12.

The direct proportionality between ion generation rate and ion current density within a plasma is a fundamental principle.

As the plasma produces more ions, there is a corresponding increase in the number of charge carriers available to contribute to the overall electric current. Figure 4 visually supports this assertion by demonstrating a positive correlation between the dielectric constant of the insulating material and the resulting ion current density. In essence, a higher dielectric constant facilitates enhanced ion generation within the plasma, thereby augmenting the ion current density.

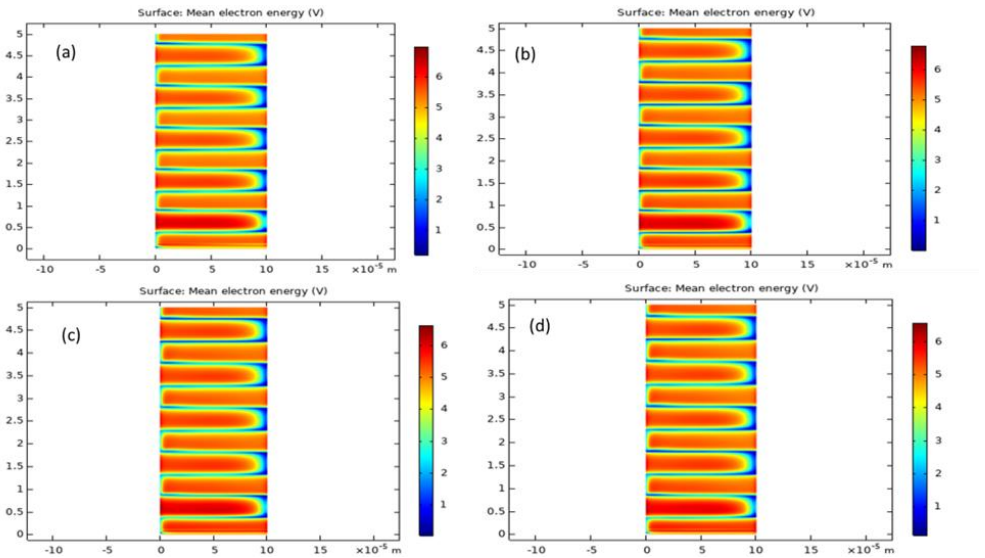

Figure 5 provides extruded visualizations of the average electron energy distribution in the discharge gap for dielectric constants ranging from 6 to 12.

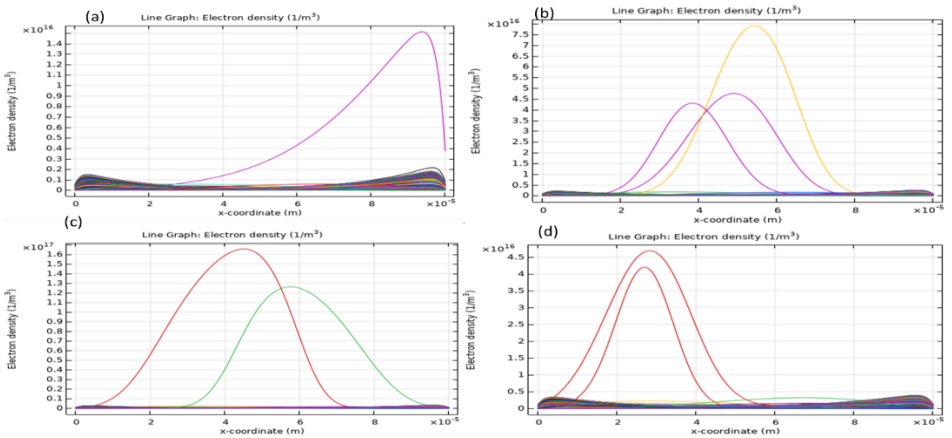

Figure 6 presents graphical representations of electron density distribution within the discharge gap at various time intervals, considering dielectric constants of 7, 8, 9, and 10.

Despite influencing the electric field intensity and other processes, variations in the dielectric constant have a minimal impact on the average electron energy. As depicted in Figure 5, the consistency of the average electron energy suggests that mechanisms affecting electron energy counteract the effects of changes in the dielectric constant.

4. CONCLUSION

A numerical study was conducted to examine how changing the dielectric constants of insulating materials affects the properties of plasma in an atmospheric pressure DBD reactor. The findings revealed that the dielectric constant is a key factor that significantly influences the spatial distribution of plasma, electric field intensity, electron density, and other discharge characteristics.Substantial changes in plasma properties were observed with alterations in the dielectric constant value. These findings underscore the critical role of selecting suitable insulating materials with optimal dielectric constants in the design and performance of (DBD) reactors. Considering the outcomes of this research, (DBD) reactors can be designed to achieve enhanced performance in various applications. For instance, by choosing insulating materials with appropriate dielectric constants, plasma distribution can be optimized, electric field intensity can be controlled, and consequently, the efficiency of plasma processes can be improved. Overall, the results of this study represent a significant step toward a better understanding of the physical mechanisms governing (DBD) reactor plasmas and the optimal design of these reactors for diverse applications.

REFERENCES

[1]M. M. Nasiru, E. B. Frimpong, U. Muhammad, J. Qian, A. T. Mustapha, W. Yan, H. Zhuang and J. Zhang, Compr. *Impact of dielectric barrier discharge cold plasma on the lipid oxidation, color stability, and protein structures of myoglobin-added washed pork muscle*. Rev. Food Sci. Food Saf, 20, 2626 (2021). https://doi.org/10.3389/fnut.2023.1137457.

[2]R. Snoeckx and A. Bogaerts, Plasma technology – a novel solution for CO2 conversion. Chem. Soc. Rev 46, 5805 (2017). https://doi.org/10.1039/C6CS00066E.

[3] A. H. Khoja, M. Tahir and N. A. S. Amin, *Recent developments in nonthermal catalytic DBD plasma reactor for dry reforming of methane*. Energy convers. manage, 183, 529-560 (2019). https://doi.org/10.1016/j.enconman.2018.12.112.

[4] N. Dadashzadeh and E. Poorreza, *Comparative analysis and simulation of a dielectric discharge barrier reactor using the finite element method*, Quarterly Journal of Optoelectronic 6 (3), 7-16 (2024).

https://doi.org/10.30473/jphys.2024.69563.1172.

[5] E. Poorreza and N. Dadashzadeh Gargari, *Computational Study of an Inductively Coupled Plasma with Different Copper Coil Designs and Dielectric Thickness,* Russian Journal of Physical Chemistry A 98, pp. 249256. (2024). https://doi.org/10.1134/S0036024424050224.

[6] E. Poorreza and N. Dadashzadeh, *Modeling and Finite element analysis of argon gas plasma produced by inductively coupled plasma method with variable input power, coil position and dielectric thickness*, Quarterly Journal of Optoelectronic6(1),33-40(2023). https://doi.org/10.1134/S1990793123030235.

[7] Noushin Dadashzadeh. *Optimization of Electricity Consumption using Dielectric Barrier Discharge Method (DBD),* Majlesi Journal of Electrical Engineering 17 (1), 117-121 (2023). https://doi.org/10.30486/mjee.2023.1975011.1024.

[8] E. Poorreza and N. Dadashzadeh Gargari, *Modeling and simulation of a microwave-assisted plasma with different input power for plasma-based applications,* Russ. J. Phys. Chem. B 17 719–724 (2023). https://doi.org/10.1134/S1990793123030235.

[9] G. Neretti, A. Popoli, S.G. Scaltriti, *A. Cristofolini, Real Time Power Control in a High Voltage Power Supply for Dielectric Barrier Discharge Reactors: Implementation Strategy and Load Thermal Analysis, Electronics*, 11(10) (2022) 1536. https://doi.org/10.3390/electronics11101536.

[10] A. M. Lopez, H. Piquet, D. Patino, R. Diez and X. Bonnin, *Parameters identification and gas behavior characterization of DBD systems*, IEEE Trans plasma sci 41, 2335 (2013). https://doi.org/10.1109/TPS.2013.2273462.

[11] N. Jidenko, C. Jimenez, F. Massines, J. Borra, *Nano - particle size dependent charging and electro - deposition in dielectric barrier discharges at atmospheric pressure for thin SiOx film deposition*, Journal of Physics D: Applied Physics, 40(14) (2007) 4155. https://doi.org/ 10.1088/0022-3727/40/14/009.

[12] F. Sohbatzadeh and H. Soltani, *Time-dependent one-dimensional simulation of atmospheric dielectric barrier discharge in N2/O2/H2O using COMSOL Multiphysics,* Journal of Theoretical and Applied Physics, vol. 12, no. 1, pp. 5363, 2018. https://doi.org/ 10.1007/s40094-018-0281-4.

[13] S. Das, G. Dalei, A. Barik, *A dielectric barrier discharge (DBD) plasma reactor: An efficient tool to measure the sustainability of non -thermal plasmas through the electrical breakdown of gases, in: IOP Conference Series: Materials Science and Engineering,* IOP Publishing, 2018, pp. 012004. https://doi.org/ 10.1088/1757-899X/410/1/012004.

[14] E. Poorreza and N. Dadashzadeh Gargari, *Study of the Time Dependence and One Dimensional Simulation of a Dielectric Barrier Discharge Reactor Driven by Sinusoidal High-Frequency Voltage*, Russ. J. Phys. Chem. B 17 (3) (2023). DOI:10.1134/S1990793123030107.